Journal of Medicinal Chemistry

Article

Potent Proteasome Inhibitors Derived from the Unnatural Cis-Cyclopropane Isomer of Belactosin A: Synthesis, Biological Activity, and Mode of Action

Satoshi Shuto, Shuhei Kawamura, Yuka Unno, Anja List, Takuma Sasaki, Motohiro Tanaka, Mitsuhiro Arisawa, Akira Asai, and Michael Groll

J. Med. Chem., **Just Accepted Manuscript** • DOI: 10.1021/jm4002296 • Publication Date (Web): 02 Apr 2013

Potent Proteasome Inhibitors Derived from the Unnatural *Cis*-Cyclopropane Isomer of Belactosin A: Synthesis, Biological Activity, and Mode of Action

Shuhei Kawamura,[a,#] Yuka Unno,[b,#] Anja List,[c] Motohiro Tanaka,[d] Takuma Sasaki,[d] Mitsuhiro Arisawa,[a] Akira Asai,[b] Michael Groll,[c] and Satoshi Shuto*,[a].

[a]Faculty of Pharmaceutical Sciences, Hokkaido University, Kita-12, Nishi-6, Kita-ku, Sapporo 060-0812, Japan

[b]Graduate School of Pharmaceutical Sciences, University of Shizuoka, Yada, Shizuoka 422-8526, Japan

[c]Center for Integrated Protein Science at the Department of Chemistry, Chair of Biochemistry, Technische Universität München, Lichtenbergstrasse 4, 85747 Garching, Germany

[d]School of Pharmacy, Aichi Gakuin University, 1-100 Kusumoto-cho, Chikusa-ku, Nagoya 464-8650, Japan

Corresponding Author: Satoshi Shuto

Phone & Fax: +81-11-706-3769. E-mail: shu@pharm.hokudai.ac.jp

[#]These authors contributed equally.

Abstract

The natural product belactosin A (**1**) with a *trans*-cyclopropane structure is a useful prototype compound for developing potent proteasome (core particle, CP) inhibitors. To date, **1** and its analogs are the only CP ligands bind to both the

non-primed S1 pocket as well as the primed substrate binding channel, however, these molecules harbor a high IC_{50} value of more than 1 μM. We have performed structure activity relationship studies, hereby elucidating unnatural *cis*-cyclopropane derivatives of **1** that exhibit high potency to primarily block the chymotrypsin-like active site of the human constitutive (cCP) and immunoproteasome (iCP). The most active compound **3e** reversibly inhibits cCP and iCP similarly with an IC_{50} of 5.7 nM. X-ray crystallographic analysis of the yeast proteasome in complex with **3e** revealed that the ligand accommodates predominantly to the primed substrate binding channel and covalently binds to the active site threonine residue *via* its β-lactone ring-opening.

Introduction

The ubiquitin-proteasome system is the major pathway for systematic degradation of intracellular proteins[1] and involved in many physiologically important cellular processes such as signal transduction[2], immune reponse[3] or cell cycle progression.[4] Since proteasome inhibition causes cell cycle arrest and induces apoptosis, the 20S proteasome core particle (CP) is an attractive target molecule of anticancer drugs and autoimmune disorders.[5] In fact, the dipeptide boronic acid bortezomib (Figure 1) is in our days a prescriptive drug against various cancer types and currently represents the best known blockbuster with annual sales of more than $ 1 Mrd.[6]

Eukaryotic CPs contain three active β subunits (β1, β2, and β5, which are responsible for the caspase-like (C-L), trypsin-like (T-L) and chymotrypsin-like (ChT-L) activity, respectively),[7] whereas vertebrates present an even more elaborate version of proteasomes,[8] harboring three different types of the CP, the constitutive (cCP), immuno (iCP) and thymoproteasome (tCP), which all of them have their own set of active sites[9]: the cCP incorporates subunits β1c, β2c, and β5c, the iCP β1i, β2i, and β5i, and the tCPs β1i, β2i, and β5t. The mechanism of peptide bond cleavage follows a

universal principle among all active sites, however, it is the singularity of each substrate binding channel which determines the chemical nature of the specificity (S) pockets and accommodates the ligand's side chains (P sites) in respect to their amino acid progression. Interestingly, the iCP is induced by interferon-γ and primarily expressed in hematopoietic cells[10] while the cCP is expressed in all kind of cells. Thus, it is a well-known fact that blocking either the cCP or iCP has a major impact on specific biological potencies.[3, 5a]

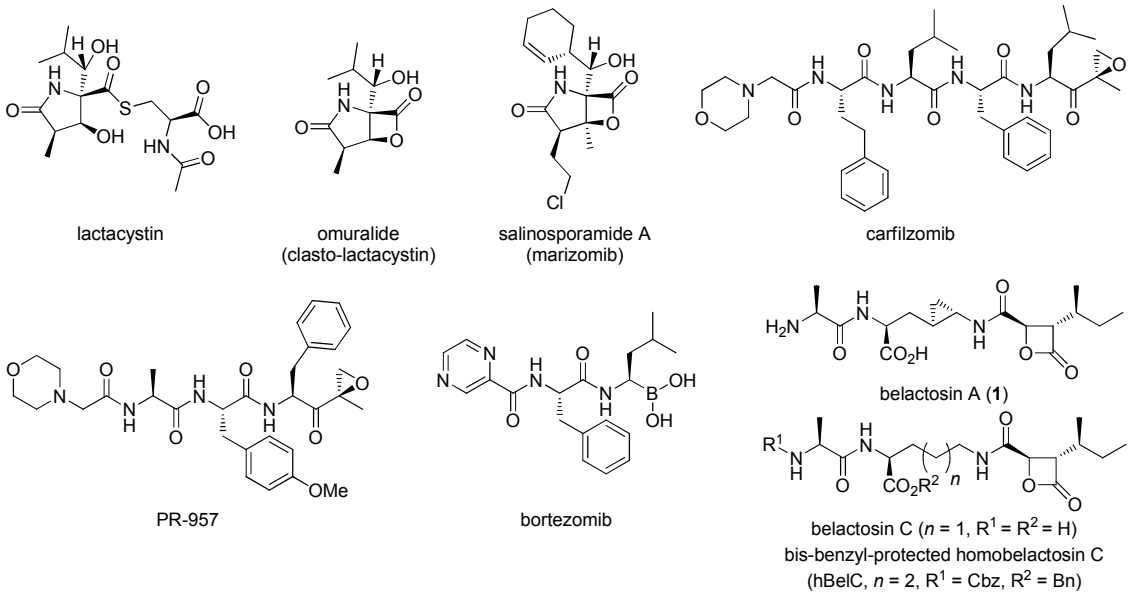

Figure 1. Known proteasome inhibitors.

Belactosin A (**1**), which is a naturally occurring *Streptomyces sp.* tripeptide metabolite and consists of L-alanine, 3-(*trans*-2-aminocyclopropyl)-L-alanine (*trans*-3,4-methano-L-ornithine) as well as a chiral carboxy-β-lactone moiety, was initially identified as a CP inhibitor by Asai and co-workers.[11] It prevents cell cycle division in tumor cells at the G2/M stage due to its proteasomal inhibition and is therefore a novel lead for developing potent anticancer agents.[11b] Inactivation of the CP by belactosin A takes place by acylation of the active site threonine 1 (Thr1) residue *via*

ring-opening of its strained β-lactone, as confirmed by X-ray crystallographic analysis of bis-benzyl-protected homobelactosin C (hBel) bound to the yeast 20S proteasome (yCP).[12] Furthermore, the structural investigations of the yCP:hBel complex revealed that the inhibitor occupies the S1 specificity pocket with its (*S*)-*sec*-butyl side chain (pseudo-isoleucine) whereas the remaining part of the ligand points towards the primed substrate binding site,[12] contrary to all currently identified CP inhibitors.[13] Although many structure-activity relationship (SAR) studies of proteasome ligand complexes have been reported, there exists only limited knowledge of inhibitors binding to the primed substrate binding channel.[12b] Thus, detailed analysis using belactosin analogs as a prototype are important to exploit both, the primed and non-primed specificity channels as presented in this work.

The class of belactosins all harbors a cyclopropan, a chemical moiety that is extensively used in medicinal chemistry due to their unique steric and electronic properties and their ability to function as alkene bioisosteres without the associated metabolic liability.[14] Since the impact of the cyclopropane in these natural products has so far not been addressed, we aimed to characterize the restriction of the orientation of the L-Ala and the key β-lactone moieties by including this ring-motif and to address its binding profile and mode of action by elucidating the three-dimensional structure of the ligand in complex with the yCP. We thus designed and synthesized a series of belactosin A derivatives with stereochemical diversity in which the central aminocyclopropyl-L-alanine (methano-L-ornithine) part was substituted with a corresponding stereo- or regioisomeric unnatural cyclopropane amino acid. Principal focus was to clarify that the *cis*/L-*anti*-isomer **2** (Figure 2) exhibiting the cyclopropane structure in *cis*-configuration is a more potent proteasome inhibitor than the natural belactosin A having the cyclopropane structure in *trans*.[15]

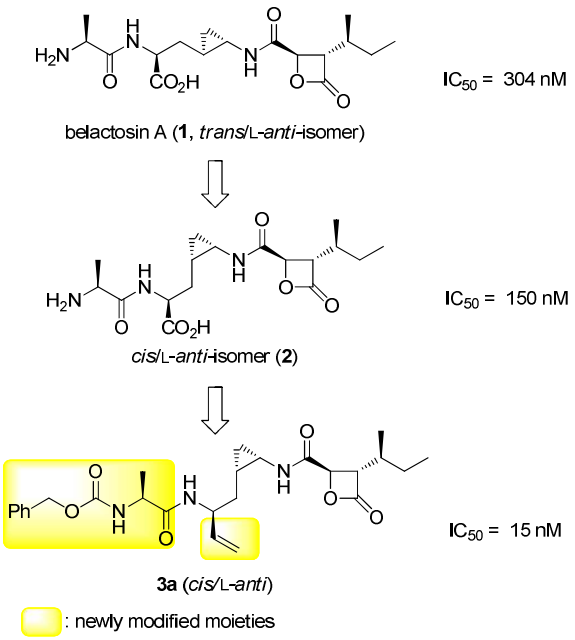

Figure 2. Proteasome inhibitors developed by us using belactosin A as a prototype.

Applying systematic SAR studies on the primed substrate binding site by using the originally identified *cis*-cyclopropane analog of belactosin A as the lead compound, we looked for highly potent compounds, whose proteasome inhibitory activities are comparable to those of bortezomib[16] and carfilzomib.[17] Furthermore, we investigated various biological properties of the developed synthetic molecules, such as selectivity for constitutive CP subunits, inhibitory effects on the subunit β5i, cell-growth inhibition and stability. Furthermore, the covalent binding mode of the designed inhibitors was clarified by applying X-ray crystallographic analysis using the yCP.

Results and Discussion

Design of Compounds. A comparison of the structure of **3a**[18] with that of **2** reveals that the carboxy group is replaced with a vinyl group and a Cbz group is introduced into the terminal amino group of the Ala moiety (Figure 2). This structural change was thought to make **3a** more potent than **2**, and we therefore aimed to modify these two moieties

further to investigate the SAR in detail. Thus, we synthesized new compounds **4a-17a** (Figure 3-a), in which the terminal Ala moiety of **3a** was replaced with a variety of acyl and amino acyl groups as well as other new compounds **3b-j** (Figure 3-b), in which the vinyl group of **3a** was substituted by hydrophobic groups such as ethyl, phenyl or alkyl-tethered aromatic rings. Furthermore, we created compounds **7e** and **16e** (Figure 3-c) having a phenethyl group at the vinyl moiety of **3a** significantly alters the CP binding profile as described in detail below.

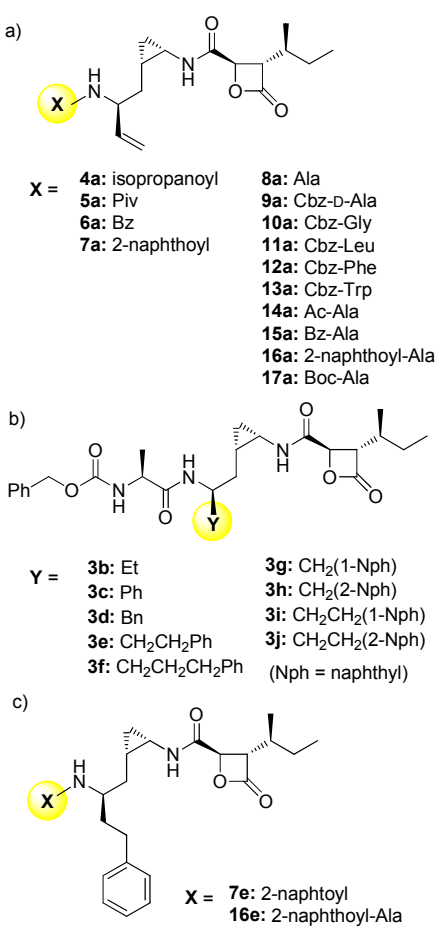

Figure 3. Newly designed compounds as proteasome inhibitors.

Synthesis. We previously developed the chiral cyclopropane units consisting of a *cis*-unit **18** (Scheme 1), its *trans*-isomer, and their two enantiomers, which are highly effective for a series of stereochemically diverse

cyclopropane compounds.[14b-d, 19] In fact, these units allowed for the productive synthesis of a series of stereo- and regioisomers of belactosin A[15] and identified the lead compound **3e**[18] with significant proteasome inhibitory potency (see below).

In this study, all of the target compounds (Figure 3) were prepared using the *cis*-unit **18**. As summarized in Scheme 1, after conversion of the unit **18** into the (*S*)-*t*-butanesulfinyl imine **19**,[15] its reaction with various Grignard reagents afforded the corresponding adduct **I** diastereoselectively, which could be further converted into **II** *via* Curtius rearrangement. The target compounds **III** were obtained from **II** by condensation with the known chiral carboxy-β-lactone[20] and acylation of the terminal amino group.

Scheme 1. Synthetic plan of target compounds

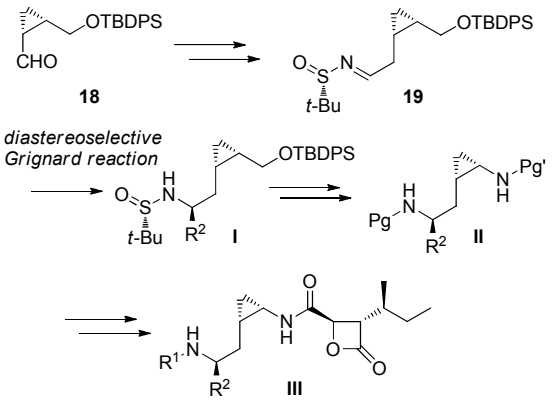

A large amount of the *cis*-unit **18** in high optical purity was required and we focused on the method reported by Charette:[21] the chiral *cis*-alcohol **21** was enantioselectively prepared applying an asymmetric Simmons-Smith reaction of a 2-butenediol derivative **20** using a chiral ligand. This reaction was suitable for large-scale synthesis, and we successfully prepared about 30 g of **21** (quantitative yield) in 92% ee. Furthermore, we found that, after Swern oxidation of **21**, the desired unit **18** was obtained in 98% ee by recrystallization from hexane (Scheme 2).

Scheme 2. Synthesis of chiral cyclopropane unit **18** with high optical purity

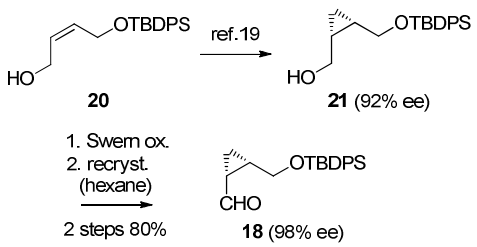

Having enough compound **18** available, we next synthesized the *N*-substituted target compounds **4a-17a** (*N*-Boc-protected compound **26a** was the common intermediate as shown in Scheme 3). Compound **22a**, prepared according to our previous protocol,[15] was converted into the aldehyde **23a**. After Pinnick oxidation of **23a**, the resulting carboxylic acid was treated with diphenyl phosphoryl azide (DPPA)/Et_3N in CH_2Cl_2 to form the corresponding acyl azide. A Curtius rearrangement yielded the cyclopropylamine derivative **24a**. Condensation of **24a** and the known β-lactone unit **25**[20] afforded **26a**. After removal of the Boc group of **26a**, *N*-acylation with acid chlorides gave the target compounds **4a-7a**. The *N*-aminoacyl-type target compounds **9a-13a** and **17a** were obtained by applying the mixed anhydride method. Compounds **8a** and **14a-16a** were prepared from **17a**.

Scheme 3. Synthesis of target compounds **4a-17a** and **3b**[a]

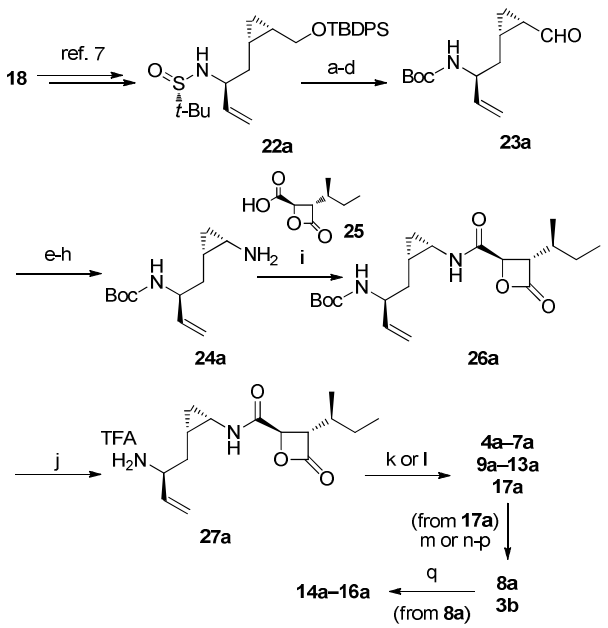

[a]Reagents and conditions: (a) HCl, THF/H_2O, 0 °C; (b) Boc_2O, Et_3N, THF; (c) TBAF, THF; (d) Swern ox., 66% (4 steps); (e) Pinnick ox.; (f) DPPA, Et_3N, CH_2Cl_2, 0 °C to rt; (g) toluene, reflux; (h) KOH, THF/H_2O; (i) **25**, PivCl, Et_3N, CH_2Cl_2, 0 °C to rt, 48% (5 steps); (j) TFA, CH_2Cl_2, 0 °C to rt; (k) RCl, Et_3N, CH_2Cl_2, 0 °C, yields (2 steps) were as follows respectively, **4a** (R = isopropanoyl) quant., **5a** (R = Piv) 81%, **6a** (R = Bz) 78%, **7a** (R = 2-naphthoyl) 92%; (l) R-OH, PivCl, Et_3N, CH_2Cl_2, 0 °C, yields (2 steps) were as follows respectively, **9a** (R = Cbz-D-Ala) quant., **10a** (R = Cbz-Gly) 96%, **11a** (R = Cbz-Leu) 64%, **12a** (R = Cbz-Phe) 66%, **13a** (R = Cbz-Trp) 65%, **17a** (R = Boc-Ala) quant.; (m) TFA, CH_2Cl_2, 0 °C, quant. (**8a**); (n) Pd/C, H_2, THF; (o) TFA, CH_2Cl_2, 0 °C; (p) CbzCl, Et_3N, CH_2Cl_2, 0 °C, 66% (3 steps, **3b**); (q) RCl, Et_3N, CH_2Cl_2, 0 °C, yields were as follows respectively, **14a** (R = Ac) 59%, **15a** (R = Bz) quant., **16a** (R = 2-naphthoyl) 95%.

Compounds **3c-j** (Figure 3-b), which have various hydrophobic groups instead of the vinyl moiety were synthesized successively, following the protocol for **3a** as shown in Scheme 4[15, 18]; the ethyl derivative **3b** was obtained *via*

hydrogenation of **17a** (Scheme 3). The synthesis of **7e** and **16e** is shown in Scheme 5 and Scheme 6, respectively.

Scheme 4. Synthesis of target compounds **3c-j**[a]

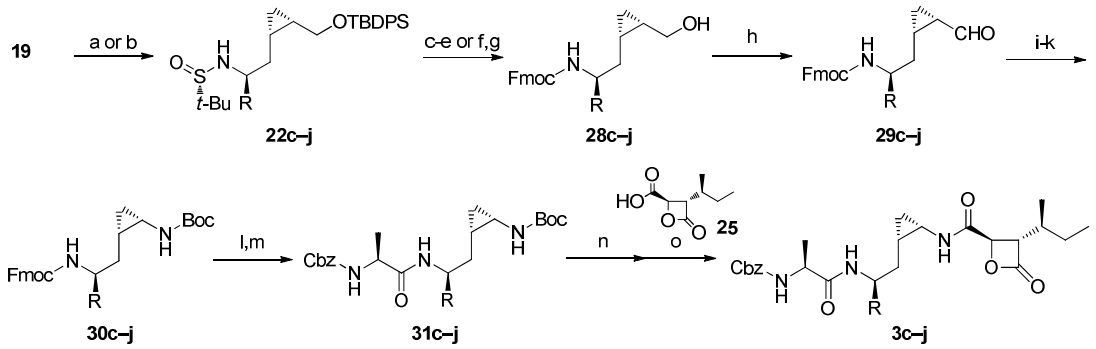

[a]Reagents and conditions: (a) RMgX, toluene, reflux; (b) RMgX, CH_2Cl_2; (c) HCl, THF/H_2O, 0 °C; (d) FmocOSu, Na_2CO_3, THF/H_2O; (e) HCl, AcOEt/MeOH, yields (4 steps) were as follows, respectively, **28c** (R = Ph) 60%, **28d** (R = Bn) 56%, **28e** (R = phenethyl) 35%, **28f** (R = phenylpropyl) 26%; (f) HCl, AcOEt/MeOH; (g) FmocOSu, Na_2CO_3, THF/H_2O, yields (3 steps) were as follows respectively, **28i** (R = 1-naphthylethyl) 36%, **28j** (R = 2-naphthylethyl) 48%; (h) DMP, CH_2Cl_2, yields (4 steps) were as follows respectively, **29g** (R = 1-naphthylmethyl) 20%, **29h** (R = 2-naphthylmethyl) 20%; (i) Pinnick ox.; (j) DPPA, Et_3N, CH_2Cl_2, 0 °C to rt; (k) *t*-BuOH, reflux, yields (4 steps for **30c-f**,**i**,**j** and 3 steps for **30g**,**h**) were as follows respectively, **30c** (R = Ph) 70%, **30d** (R = Bn) 74%, **30e** (R = phenethyl) 70%, **30f** (R = phenylpropyl) 62%, **30g** (R = 1-naphthylmethyl) 64%, **30h** (R = 2-naphthylmethyl) 64%, **30i** (R = 1-naphthylethyl) 59%, **30j** (R = 2-naphthylethyl) 52%; (l) K_2CO_3, MeOH; (m) Cbz-Ala-OH, PivCl, Et_3N, CH_2Cl_2, 0 °C to rt, yields (2 steps) were as follows respectively, **31c** (R = Ph) 74%, **31d** (R = Bn) 70%, **31e** (R = phenethyl) 84%, **31f** (R = phenylpropyl) 88%, **31g** (R = 1-naphthylmethyl) 97%, **31h** (R = 2-naphthylmethyl) 89%, **31i** (R = 1-naphthylethyl) 94%, **31j** (R = 2-naphthylethyl) 98%; (n) TFA, CH_2Cl_2; (o) **25**, PivCl, Et_3N, CH_2Cl_2, 0 °C to rt, yields (2 steps) were as follows respectively, **3c** (R = Ph) 100%, **3d** (R = Bn) 100%, **3e** (R = phenethyl) 86%, **3f** (R =

phenylpropyl) 87%, **3g** (R = 1-naphthylmethyl) 74%, **3h** (R = 2-naphthylmethyl) 82%, **3i** (R = 1-naphthylethyl) 76%, **3j** (R = 2-naphthylethyl) 83%.

Scheme 5. Synthesis of target compound **7e**[a]

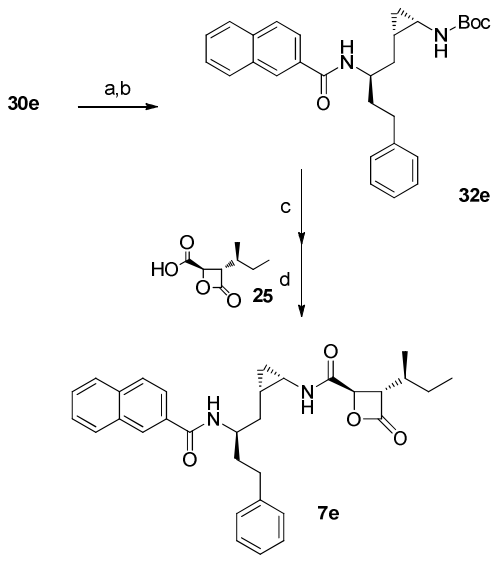

[a]Reagents and conditions: (a) K_2CO_3, MeOH; (b) 2-naphthoyl chloride, Et_3N, CH_2Cl_2, 0 °C; (c) TFA, CH_2Cl_2; (d) **25**, PivCl, Et_3N, CH_2Cl_2, 0 °C to rt, 48% (4 steps).

Scheme 6. Synthesis of target compound **16e**[a]

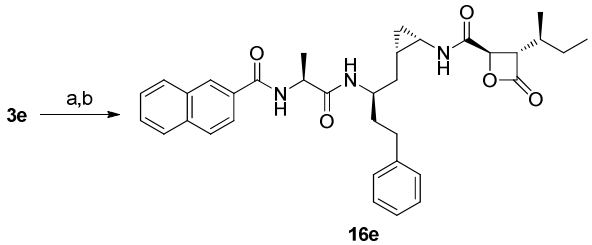

[a]Reagents and conditions: (a) Pd/C, H_2, TFA/THF, 0 °C; (b) 2-naphthoyl chloride, Et_3N, CH_2Cl_2 0 °C, 76% (2 steps).

Inhibitory effect on the ChT-L activity of human cCP. The inhibitory effect of compounds on the ChT-L activity of

human 20S proteasomes was measured using the chromophoric substrate Suc-LLVY-AMC. The results for the compounds **4a-17a** modified at the Ala moiety of the lead compound **3a** are summarized in Table 1.[22] Interestingly, modifications of the Ala moiety in the ligands exhibit a strong effect on the proteasome inhibition profiles with IC_{50} values ranging between 25 - 300 nM. The inhibitory effects of the *N*-acylated compounds **4a**, **5a**, and **6a** were weak (IC_{50} = 130-230 nM) due to the lack of the alanine-moiety, while the *N*-(2-naphthoyl) compound **7a** could compensate this absence and recapture its potent inhibitory effect (IC_{50} = 60 nM). Removal of the hydrophobic Cbz group in **3a**, i.e. the *N*-alanyl derivative **8a**, significantly decreased the activity due to lack of the hydrophobic interaction (IC_{50} = 300 nM).

Compounds **9a-13a**, in which the Cbz-L-Ala of **3a** was replaced with other Cbz-amino acids, exhibited inhibitory effects (IC_{50} = 28-57 nM) comparable to **3a** (IC_{50} = 49 nM). The *N*-substituted alanyl compounds, *N*-Bz-Ala (**15a**), *N*-(2-naphthoyl)-Ala (**16a**), and *N*-Boc-Ala (**17a**) derivatives, were shown to be potent inhibitors (IC_{50} = 25-79 nM), while the *N*-Ac-Ala derivative **14a** had a decreased binding profile (IC_{50} = 230 nM).

These systematic SAR studies focused on the Ala moiety suggested that Ala structure is not essential for the high potency (**3a** versus 7**a**, **9a-13a**) but it seems to function as a linker to place a hydrophobic group attached at the terminal amino group into the proteasome hydrophobic binding pocket (**5a** versus **17a**). Compound **7a** does not include Ala structure but its large *N*-(2-naphthoyl) group might enable itself to reach the hydrophobic binding pocket. Also as the hydrophobic moiety, not only an aromatic group but also an aliphatic hydrophobic group, as exemplified by **17a**, can be accommodated in the pocket. Thus, potency of the proteasome inhibition by the compounds summarized in Table 1 would reflect the efficacy of the hydrophobic interactions with the pocket.

Among them, the *N*-(2-naphthoyl)-Ala derivative **16a** (IC_{50} = 25 nM) was the most potent compound identified.

Table 1. Proteasome inhibitory effects of compounds **3a**-**17a** modified at the *N*-Cbz-alanyl moiety in **3a**.

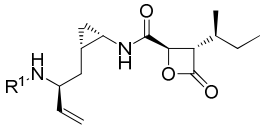

compound number	R^1	ChT-L activity, IC_{50} [nM][a]
3a	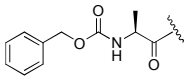	49 ± 9.5
4a		230 ± 40
5a		210 ± 25
6a		130 ± 13
7a	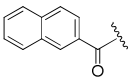	60 ± 12
8a		300 ± 70
9a	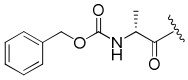	57 ± 12
10a	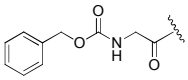	41 ± 11
11a	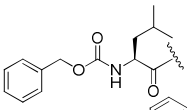	47 ± 9.2
12a	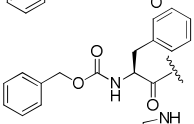	30 ± 3.1
13a	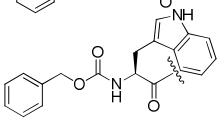	28 ± 2.6
14a	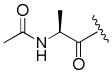	230 ± 35
15a	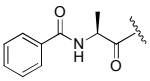	79 ± 13
16a	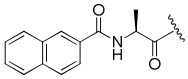	25 ± 1.7
17a	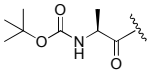	77 ± 12

belactosin A	1440
bortezomib	4.5

[a]Based on three experiments.

Due to the lack of structural insights of substrate binding into the primed sites of the CP we performed an analytical random screen at the vinyl moiety of **3a**, which is summarized in Table 2. Notably, this site turned out to have a significant effect on the IC_{50} of each of the synthesized compound varying between 5.7 and 200 nM. The order of the inhibitory potency of these compounds is according to: **3e** > **3d** > **3j** > **3f** > **3b** > **3a** > **3i** > **3c** > **3g** > **3h**. Introduction of a phenyl ring clearly improved the inhibitory activity, in which the best side chain length was identified to be two carbons (n = 2), i.e. the phenethyl derivative **3e**. The IC_{50} value of **3e** was as low as 5.7 nM and comparable to that of the clinical drug bortezomib (IC_{50} = 4.5 nM).

Table 2. Proteasome inhibitory effects of compounds **3a-j** modified at the vinyl moiety in **3a**.

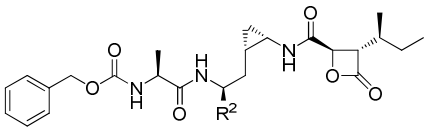

compound number	R^2	ChT-L activity, IC_{50} [nM][a]
3a		49 ± 9.5
3b		38 ± 11
3c		90 ± 20
3d		14 ± 1.2

3e	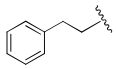	5.7 ± 1.2
3f	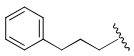	35 ± 9.1
3g	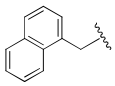	130 ± 17
3h	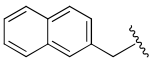	200 ± 44
3i	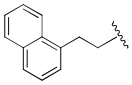	63 ± 10
3j	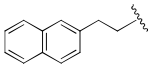	29 ± 7.8
belactosin A		1440
bortezomib		4.5

[a]Based on three experiments.

Finally, we designed phenethyl-type compounds **7e** and **16e**, where 2-naphthoyl and 2-naphthoyl-Ala groups were selected as potentially effective *N*-substituents based on the results summarized in Table 1, respectively (Table 3). Both of these compounds revealed superb IC_{50} values of 33 nM (**7e**) and 10 nM (**15e**), respectively, as explained by the structural results (see below).

Table 3. Proteasome inhibitory effects of compounds **7e** and **16e** modified at the *N*-Cbz-alanyl moiety in **3e**.

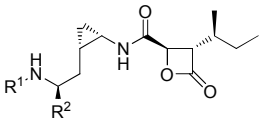

compound number	R^1	R^2	ChT-L activity, IC_{50} [nM][a]
3a	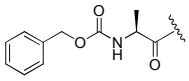		49 ± 9.5

7e	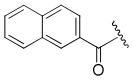	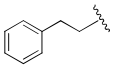	33 ± 8.4
16e	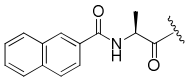	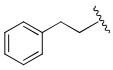	10 ± 1.0
belactosin A			1440
Bortezomib			4.5

[a]Based on three experiments.

Inhibitory effects on the C-L and T-L activities on human cCP and other proteases. Next, we evaluated the inhibitory activity of the selected compounds (**3a**, **7a**, **12a**, **16a**, **3e** and **16e**) against the C-L (β-1) and T-L (β-2) activities of the human cCP using Ac-*n*LP*n*LD-AMC and Ac-RLR-AMC as chromophoric substrates, respectively. As summarized in Table 4, all these compounds inhibit the C-L activity > 600 nM (Table 4) in agreement to belactosin analogs,[11b, 12] suggesting that C-L inhibition at high concentrations is a common property of this class of proteasome ligands whereas the T-L active sites is not altered >1300 nM (see structural results). It has been reported that bortezomib inhibits beside the proteasome as a major target also a multitude of serine proteases, thus causing severe side effects upon application.[23] Contrary, evaluation of the inhibitory activity of **3e** against proteases such as caspase 3, cathepsin B and trypsin revealed strong selectivity for the CP and therefore supports further optimization of this class of compounds for future drug development (Figure 4).

Table 4. Inhibitory activity of selected compounds against ChT-L, C-L and T-L activity of proteasomes and cell growth.

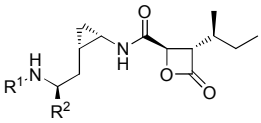

compound number	R^1	R^2	IC_{50} [nM][a]			cell growth IC_{50} [μM]
			ChT-L activity	C-L activity	T-L activity	HCT116
3a	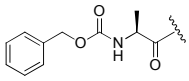		49 ± 9.5	1600	> 3000	0.91
7a	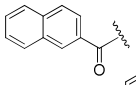		60 ± 1.2	670	1900	11.2
12a	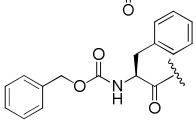		30 ± 3.1	1780	2190	4.16
16a	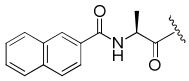		25 ± 1.7	690	1320	2.61
3e	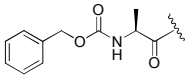	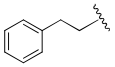	5.7 ± 1.2	2420	1920	1.82
16e	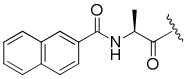	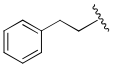	10 ± 1.0	> 3000	> 3000	0.79
bortezomib			4.5	130	1880	0.01

[a]Based on three experiments.

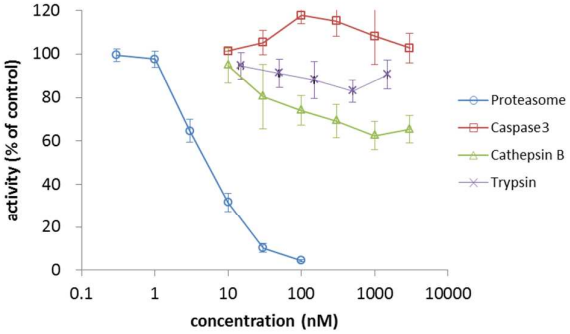

Figure 4. Effect of **3e** on various proteases compared to the CP.

Inhibitory effects on human β5i of the iCP. New studies on the selective inhibition of the iCP demonstrated a

therapeutic benefit, particularly in autoimmune diseases and put the iCP in the limelight as a novel drug target.[5a, 9a, 24] Yet, there have been no reports on the binding properties of the class of belactosins and its derivatives to the immunoproteasome. We thus evaluated the inhibitory effects of belactosin A and **3e** on human β5i *via* an active-site ELISA method according to Kuhn et al.[17b] Bortezomib, lactacystin and PR-957 were used as controls beside analysis of belactosin A and **3e**. Figure 5 displays the binding profile for each of the compounds for the human cCP and iCP. Remarkably, lactacystin and PR-957 have a strong tendency to either inhibit β5c or β5i, respectively,[5a] whereas belactosin A and its derivative **3e** block the ChT-L sites of each CP-type equally, similar as bortezomib. These data represent for the first time a comparison on the binding probabilities of ligands which are selective for both, the non-primed and primed sites of the proteasome. Interestingly, the results demonstrate that at least **3e** do not show apparent alterations in their affinity to a specific type of the CP (see structural results).

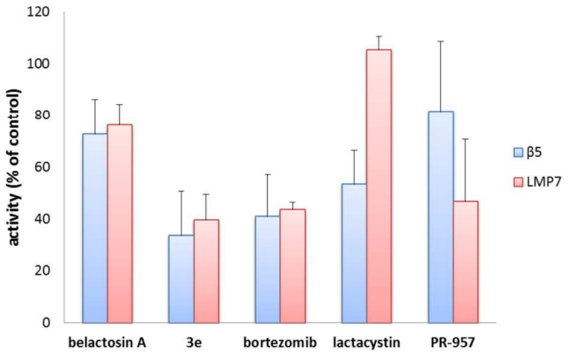

Figure 5. Active-site ELISA analysis of 20S proteasomes or 20S immunoproteasomes incubated with various inhibitors; concentration of compounds was 0.3 μM, except for lactacystin (2.5 μM).

Inhibitory Effect on Cell Growth. Next, we investigated the cell growth inhibitory effects of selected compounds (**3a**, **7a**, **12a**, **16a**, **3e**, **16e**) on HCT116. As summarized in Table 4, all of these compounds showed cell growth inhibitory

effects with IC_{50} values of 0.79 - 11.2 μM as compared to bortezomib (IC_{50} = 0.01μM). Furthermore, we examined the cell cycle distribution of HCT116 cells. As shown in Figure 6, **3e** inhibited cell cycle progression at the G2/M stage like bortezomib which is also revealed for most of the compounds (see supporting information).

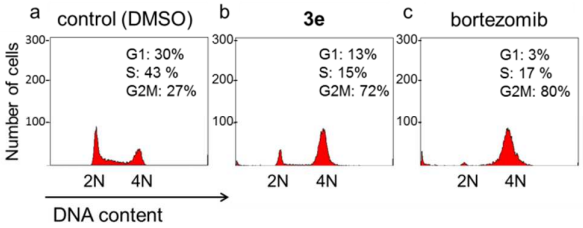

Figure 6. Cell cycle distribution analysis of HCT116 cells treated with (a) DMSO, (b) **3e** or (c) bortezomib.

In parallel, we investigated the proteasome inhibitory effect of these inhibitors in a cellular system by Western blot analysis. The tumor suppressor gene product p53 is a well-known proteasome target.[25 26] As shown in Figure 7, p53 was clearly accumulated in HCT116 cells treated with belactosin derivatives. Furthermore, cleavage of poly(ADP-ribose) polymerase (PARP), a prominent marker of apoptosis,[27] was observed in the treated cells, indicating that the apoptotic pathway is activated in the cells. These results suggest that CP blockage by our designed balactosin derivatives induces G2/M cell cycle arrest and causes an accumulation of p53, which result in HCT116 cell apoptosis, thus explaining the observed cell growth inhibitory effects.

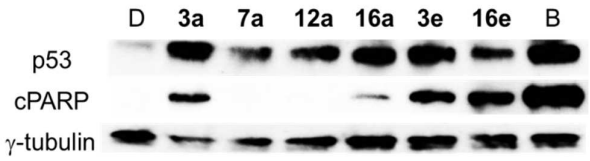

Figure 7. Immunoblot analysis of p53 and cPARP in HCT116 cells treated with bortezomib (B), belactosin derivatives

(**3a**, **7a**, **12a**, **16a**, **3e**, **16e**), or DMSO (control, D).

Stability in Aqueous Medium. So far, all potent inhibitors identified in this study were only poorly soluble in aqueous medium, thus we employed **33e** (Table 5) by removal of the *N*-terminal Cbz group in **3e**. In contrast to previous belactosin analogues, **33e** could be incubated in 0.1 M triethylammonium acetate (TEAA) buffer (pH 7.4), allowing to record a time-course by HPLC, hereby determining its half-life ($t_{1/2}$). As summarized in Table 5, the $t_{1/2}$ of **33e** in pH 7.4 buffer was approximately 10 h, indicating that it is chemically much more stable than other β-lactone type proteasome inhibitors (omuralide, 13 min; salinosporamide A, 56 min).[28]

Table 5. The chemical stability of **33e**, omuralide and salinosporamide A.

	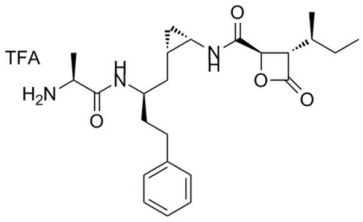 **33e**	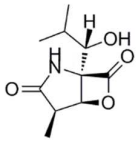 omuralide	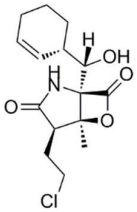 salinosporamide A
$t_{1/2}$ in pH 7.4 buffer (37 °C)	10 h	13 min[a]	56 min[a]

[a]From ref. 28

Mode of Proteasome Inhibition. An interesting approach for the conversion of a reversible into an irreversible β–lactone inhibitor is exemplified by omuralide[7] versus salinosporamide A (Sal A).[29] Sal A exhibits essentially the same scaffold as omuralide, though it displays a chloroethyl group in the P2 site. This latter moiety is responsible for the

irreversible mode of action, since after ester bond formation with Thr1O$^{\gamma}$ a second reaction occurs resulting in a tetrahydrofuran ring. Belactosins invert the classic concept of previously described β–lactone compounds as identified in the yCP crystal structure in complex with hBel.[12a] It was shown that this class of belactosins, which lack the γ-lactam-ring, bind to the CP in a reversed fashion, targeting predominantly the primed site of the substrate binding channel. To date, its mode of action to either bind reversible or irreversible has not been addressed. We therefore preincubated the CP with **3e** and measured the CP activity before and after dialysis in comparison to bortezomib and carfilzomib. As shown in Figure 8 and in agreement with previous reports[17a, 28, 30] bortezomib and carfilzomib exhibit different mode of actions to block the proteasome activity either reversible or irreversible. The inhibitory effect of **3e** was attenuated after dialysis and therefore classifies belactosines as slowly reversible CP inhibitors, however with dissociation rates even less than bortezomib.

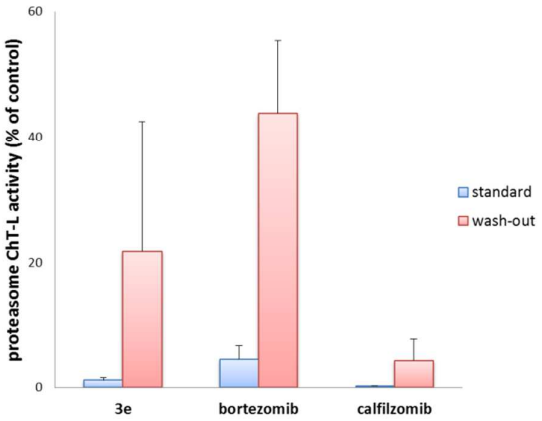

Figure 8. ChT-L activity of the 20S proteasome treated with **3e**, bortezomib and carfilzomib before and after wash-out.

Crystal structure analysis of yCP in complex with 3e. In order to gain insights into the mode of action of the newly identified highly potent *cis*-belactosin analogue, we co-crystallized **3e** with the yCP and determined its structure to 2.8

Å resolution (R_{free} = 22.4%, Table ST1). Using inhibitor concentrations in the mM range for crystal soaking experiments, the belactosin derivative targeted predominantly the β5 active sites of the yCP, whereas subunits β1 and β2 display the ligand only partially defined in the electron density map with low occupancy / high Debye-Waller factors. The improper binding profile of **3e** to the C-L and T-L sites is due to the restricted size of their primed specificity pockets as well as the sterically demanding cyclopropane group and the constrained conformation of the ligand, in agreement with the kinetic results (Table 4). Contrary, the F_o-F_c-difference electron density map of the ChT-L activity clearly depicts **3e** covalently bound by β-lactone opening and acylation of the catalytic *N*-terminal Thr1O$^{\gamma}$ as observed for the β-lactones omuralide and hBel.[7, 12a] Moreover, the (*S*)-*sec*-butyl side chain of **3e** proved to be the only side chain facing into the non-primed site as observed in the yCP:hBel complex,[12b] thus forming a multitude of Van-der-Waals interactions in the S1 specificity pocket, while the remaining part of the ligand is oriented towards the primed substrate binding channel (Figure 9-a).

In general, once bound at the active site of the CP, β-lactones generate a C4-hydroxyl group which in the case of omuralide is stabilized through a hydrogen bond with the Thr1 and occupies the position formerly taken by a nucleophilic water molecule in the unligated enzyme, hereby preventing acyl-enzyme hydrolysis by disfavoring the Bürgi-Dunitz trajectory (Figure 9-b). Contrary, **3e** performs a major structural rearrangement once bound to the yCP compared to omuralide: the newly generated hydroxyl group at C4 is H-bonded to Arg19O, hence pointing into the opposite direction, just as observed in the CP:hBel crystal structure.[12] The cyclopropane ring of **3e** adopts a position similar to that of the C4-OH of omuralide, preventing addition of the nucleophilic water molecule and thus explaining the mode of binding to act as a proteasome inhibitor, which however is different to omuralide. Notably, the binding position, the stereochemistry of **3e** and its cyclopropane ring together force the remainder of this compound into the

primed site of the CP. In agreement to the random screen for improving the binding preference towards R2 (Table 2), the phenethyl moiety is well defined in the electron density map and protrudes into a specificity pocket composed of Ser96, Tyr112, Asp114, Ser115 and Val127 of subunit β5, thus explaining its low IC_{50} value. Interestingly, most of these proteasome residues are conserved between the human cCP and iCP and thus do not distinguish between these two proteasome types in accordance with the ELISA analysis shown in Figure 5. In contrast, the Ala-moiety of **3e** is the only part of the ligand which is flexible in the crystal structure, whereas the *N*-Cbz group performs distinct Van-der-Waals interactions with Ile24 of β4 as well as Tyr129 and Phe132 of the adjacent β4'-subunit, respectively (Figure 9-a). These structural observations again confirm the functional data, showing that *N*-acyl compounds lacking the Ala-moiety can only be recaptured in their potency by introducing a spacious *N*-(2-naphtoyl) group (**7a** versus **4a**, Table 1).

Next, we performed a structural superposition of yCP bound to **3e** and hBel (Figure 9-c). Both ligands adopt a unique arrangement in the primed substrate binding channel which in some parts significantly differ to each other: though both ligands exhibit a similar binding mode to the active site Thr1O^{γ} and that of the P1 residues as well as a comparable orientation of the phenethyl side chain versus the benzyl ester moiety in hBel, the alanine moiety of the two inhibitors is oriented almost orthogonal (Figure 9-c). This unique binding of the *N*-terminal tail of **3e** is explained by the bent conformation caused by the *cis*-configuration of the cyclopropane structure, which is absent in hBel. However, the phenyl ring from the Cbz group of both ligands are directed towards a lipophilic pocket formed by the adjacent subunits β4 and β4', hereby getting stabilized by strong hydrophobic interactions. These findings coincide with the functional data showing that removal of the hydrophobic Cbz group in the belactosin derivatives increased the IC_{50} value from 49 nM (**3a**) to 300 nM (**8a**, Table 1)). Hence, the performed crystallographic studies elucidate important insights into the

design and flexibility of future proteasome inhibitors exploiting the primed substrate binding channel. Once the Thr1O$^{\gamma}$ ester bond is formed *via* the strained β-lactone opening of the ligand, stringent conformational rearrangements of the inhibitor are restricted due to the rigidity of the *cis*-cyclopropane ring linker. In addition, the binding affinity of future belactosin derivatives might be further improved by exploiting the identified hydrophilic pocket stabilizing the phenethyl side chain as well as the distal hydrophobic pocket interacting with the Cbz group of **3e**, which are both located solely in the primed substrate binding channel.

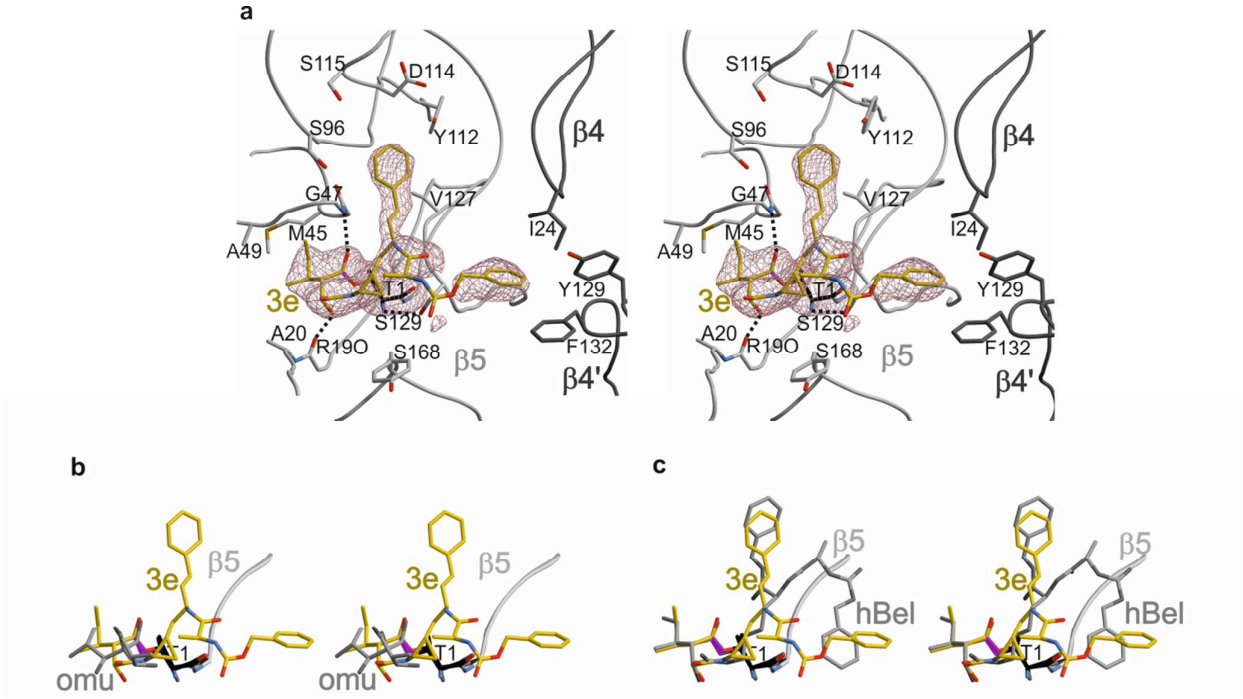

Figure 9. 3e and its binding mode to the β5 subunit. (a) Crystal structure of the ChT-L active site in complex with **3e** (PDB code 4J70). The backbone of the proteasomal subunit β5 is colored in grey, subunits β4 and β4' in dark grey, and shown in coil representation; the ligand is represented in a stick model. The $2F_o$-F_c electron density map (colored in blue), in which **3e** and Thr1 has been omitted prior phase calculations, is contoured from 1 σ (Thr1 is colored in black). The various sets of H-bonds between **3e** and β5 main chain atoms Gly47, Thr1N and Arg19O are depicted as black

dashed lines. (b) The structural superposition of **3e** and omuralide[7] as well as (c) **3e** and hBel[12a] bound to the ChT-L active site are represented in yellow and the corresponding CP-inhibitor in grey, respectively.

Conclusions

We performed the first systematic SAR study of proteasome inhibitors that bind to the primed substrate-binding site and the S1 binding site, using the unnatural *cis*-cyclopropane belactosin analog **3a** to identify a series of highly potent proteasome inhibitors. Among them, **3e** showed marked proteasome inhibitory activity as potent as bortezomib. The X-ray crystallographic analysis of the yeast proteasome in complex with **3e** revealed its covalent binding mode and allows future optimization of this interesting class of CP-inhibitors for further characterization in clinical phase studies.

Supporting Information

Supporting Information Available: Experimental details of synthesis, biological evaluation, X-ray crystallographic analysis and table listing combustion analysis data for target compounds. This material is available free of charge via the Internet at http://pubs.acs.org.

Abbreviations Used

AMC, aminomethylcoumarin; CP, core particle; DMP, Dess-Martin periodinane; ELISA, enzyme-linked

immunosorbent assay; Fmoc, 9-fluorenylmethyloxycarbonyl; HPLC, high-pressure liquid chromatography; Me, methyl; Piv, pivaloyl; Ph, phenyl; Suc, succinyl; TEAA, triethylammonium acetate; TFA, trifluoroacetic acid; THF, tetrahydrofuran

References

1. (a) Orlowski, M. The multicatalytic proteinase complex, a major extralysosomal proteolytic system. *Biochemistry* **1990**, *29*, 10289-10297; (b) Ciechanover, A. The ubiquitin-proteasome proteolytic pathway. *Cell* **1994**, *79*, 13-21.

2. (a) Fuchs, S. Y. The role of ubiquitin-proteasome pathway in oncogenic signaling. *Cancer Biol. Ther.* **2002**, *1*, 337-341; (b) Chen, J. J.; Lin, F.; Qin, Z. H. The roles of the proteasome pathway in signal transduction and neurodegenerative diseases. *Neurosci. Bull.* **2008**, *24*, 183-194.

3. Muchamuel, T.; Basler, M.; Aujay, M. A.; Suzuki, E.; Kalim, K. W.; Lauer, C.; Sylvain, C.; Ring, E. R.; Shields, J.; Jiang, J.; Shwonek, P.; Parlati, F.; Demo, S. D.; Bennett, M. K.; Kirk, C. J.; Groettrup, M. A selective inhibitor of the immunoproteasome subunit LMP7 blocks cytokine production and attenuates progression of experimental arthritis. *Nat. Med.* **2009**, *15*, 781-787.

4. King, R. W.; Deshaies, R. J.; Peters, J. M.; Kirschner, M. W. How proteolysis drives the cell cycle. *Science* **1996**, *274*, 1652-1659.

5. (a) Huber, E. M.; Groll, M. Inhibitors for the Immuno- and Constitutive Proteasome: Current and Future Trends in Drug Development. *Angew. Chem. Int. Ed.* **2012**, *51*, 8708-8720; (b) Adams, J. The proteasome: a suitable antineoplastic target. *Nat. Rev. Cancer* **2004**, *4*, 349-360.

6. (a) Bross, P. F.; Kane, R.; Farrell, A. T.; Abraham, S.; Benson, K.; Brower, M. E.; Bradley, S.; Gobburu, J. V.; Goheer, A.; Lee, S. L.; Leighton, J.; Liang, C. Y.; Lostritto, R. T.; McGuinn, W. D.; Morse, D. E.; Rahman, A.; Rosario, L. A.; Verbois, S. L.; Williams, G.; Wang, Y. C.; Pazdur, R. Approval summary for bortezomib for injection in the treatment of multiple myeloma. *Clin. Cancer Res.* **2004**, *10*, 3954-3964; (b) Kane, R. C.; Farrell, A. T.; Sridhara, R.; Pazdur, R. United States Food and Drug Administration approval summary: bortezomib for the treatment of progressive multiple myeloma after one prior therapy. *Clin. Cancer Res.* **2006**, *12*, 2955-2960; (c) Kane, R. C.; Dagher, R.; Farrell, A.; Ko, C. W.; Sridhara, R.; Justice, R.; Pazdur, R. Bortezomib for the treatment of mantle cell lymphoma. *Clin. Cancer Res.* **2007**, *13*, 5291-5294.

7. Groll, M.; Ditzel, L.; Lowe, J.; Stock, D.; Bochtler, M.; Bartunik, H. D.; Huber, R. Structure of 20S proteasome from yeast at 2.4A resolution. *Nature* **1997**, *386*, 463-471.

8. Groll, M.; Clausen, T. Molecular shredders: how proteasomes fulfill their role. *Curr. Opin. Struct. Biol.* **2003**, *13*, 665-673.

9. (a) Huber, Eva M.; Basler, M.; Schwab, R.; Heinemeyer, W.; Kirk, Christopher J.; Groettrup, M.; Groll, M. Immuno- and Constitutive Proteasome Crystal Structures Reveal Differences in Substrate and Inhibitor Specificity. *Cell* **2012**, *148*, 727-738; (b) Murata, S.; Sasaki, K.; Kishimoto, T.; Niwa, S.-i.; Hayashi, H.; Takahama, Y.; Tanaka, K. Regulation of CD8+ T Cell Development by Thymus-Specific Proteasomes. *Science* **2007**, *316*, 1349-1353.

10. Parlati, F.; Lee, S. J.; Aujay, M.; Suzuki, E.; Levitsky, K.; Lorens, J. B.; Micklem, D. R.; Ruurs, P.; Sylvain, C.; Lu, Y.; Shenk, K. D.; Bennett, M. K. Carfilzomib can induce tumor cell death through selective inhibition of the chymotrypsin-like activity of the proteasome. *Blood* **2009**, *114*, 3439-3447.

11. (a) Asai, A.; Hasegawa, A.; Ochiai, K.; Yamashita, Y.; Mizukami, T. Belactosin A, a novel antitumor antibiotic acting on cyclin/CDK mediated cell cycle regulation, produced by Streptomyces sp. *J. Antibiot.* **2000**, *53*, 81-83; (b) Asai, A.;

Tsujita, T.; Sharma, S. V.; Yamashita, Y.; Akinaga, S.; Funakoshi, M.; Kobayashi, H.; Mizukami, T. A new structural class of proteasome inhibitors identified by microbial screening using yeast-based assay. *Biochem. Pharmacol.* **2004**, *67*, 227-234.

12. (a) Groll, M.; Larionov, O. V.; Huber, R.; De Meijere, A. Inhibitor-binding mode of homobelactosin C to proteasomes: New insights into class I MHC ligand generation. *Proc. Natl. Acad. Sci. U. S. A.* **2006**, *103*, 4576-4579; (b) Korotkov, V. S.; Ludwig, A.; Larionov, O. V.; Lygin, A. V.; Groll, M.; de Meijere, A. Synthesis and biological activity of optimized belactosin C congeners. *Org. Biomol. Chem.* **2011**, *9*, 7791-7798.

13. (a) Borissenko, L.; Groll, M. 20S proteasome and its inhibitors: crystallographic knowledge for drug development. *Chem. Rev.* **2007**, *107*, 687-717; (b) Groll, M.; Kim, K. B.; Kairies, N.; Huber, R.; Crews, C. M. Crystal structure of epoxomicin : 20S proteasome reveals a molecular basis for selectivity of alpha ',beta '-epoxyketone proteasome inhibitors. *J. Am. Chem. Soc.* **2000**, *122*, 1237-1238; (c) Groll, M.; Berkers, C. R.; Ploegh, H. L.; Ovaa, H. Crystal structure of the boronic acid-based proteasome inhibitor bortezomib in complex with the yeast 20S proteasome. *Structure* **2006**, *14*, 451-456; (d) Groll, M.; Huber, R.; Potts, B. C. M. Crystal structures of salinosporamide A (NPI-0052) and B (NPI-0047) in complex with the 20S proteasome reveal important consequences of beta-lactone ring opening and a mechanism for irreversible binding. *J. Am. Chem. Soc.* **2006**, *128*, 5136-5141; (e) Groll, M.; Schellenberg, B.; Bachmann, A. S.; Archer, C. R.; Huber, R.; Powell, T. K.; Lindow, S.; Kaiser, M.; Dudler, R. A plant pathogen virulence factor inhibits the eukaryotic proteasome by a novel mechanism. *Nature* **2008**, *452*, 755-758; (f) Hines, J.; Groll, M.; Fahnestock, M.; Crews, C. M. Proteasome inhibition by fellutamide B induces nerve growth factor synthesis. *Chem. Biol.* **2008**, *15*, 501-512; (g) Clerc, J.; Groll, M.; Illich, D. J.; Bachmann, A. S.; Huber, R.; Schellenberg, B.; Dudler, R.; Kaiser, M. Synthetic and structural studies on syringolin A and B reveal critical determinants of selectivity and potency of proteasome inhibition. *Proc. Natl. Acad. Sci. U. S. A.* **2009**, *106*, 6507; (h) Blackburn, C.; Barrett, C.; Blank, J. L.; Bruzzese, F. J.; Bump, N.; Dick, L. R.; Fleming, P.; Garcia, K.; Hales, P.;

Hu, Z. Optimization of a series of dipeptides with a P3 threonine residue as non-covalent inhibitors of the chymotrypsin-like activity of the human 20S proteasome. *Bioorg. Med. Chem. Lett.* **2010**, *20*, 6581-6586; (i) Grawert, M. A.; Gallastegui, N.; Stein, M.; Schmidt, B.; Kloetzel, P. M.; Huber, R.; Groll, M. Elucidation of the alpha-keto-aldehyde binding mechanism: a lead structure motif for proteasome inhibition. *Angew. Chem. Int. Ed. Engl.* **2011**, *50*, 542-544; (j) Gallastegui, N.; Beck, P.; Arciniega, M.; Huber, R.; Hillebrand, S.; Groll, M. Hydroxyureas as Noncovalent Proteasome Inhibitors. *Angew. Chem. Int. Ed.* **2012**, *51*, 247-249; (k) Huber, E. M.; Basler, M.; Schwab, R.; Heinemeyer, W.; Kirk, C. J.; Groettrup, M.; Groll, M. Immuno-and Constitutive Proteasome Crystal Structures Reveal Differences in Substrate and Inhibitor Specificity. *Cell* **2012**, *148*, 727-738.

14. (a) Armstrong, P. D.; Cannon, J. G.; Long, J. P. Conformationally Rigid Analogues of Acetylcholine. *Nature* **1968**, *220*, 65-66; (b) Kazuta, Y.; Hirano, K.; Natsume, K.; Yamada, S.; Kimura, R.; Matsumoto, S.; Furuichi, K.; Matsuda, A.; Shuto, S. Cyclopropane-based conformational restriction of histamine. (1S,2S)-2-(2-aminoethyl)-1-(1H-imidazol-4-yl)cyclopropane, a highly selective agonist for the histamine H3 receptor, having a cis-cyclopropane structure. *J. Med. Chem.* **2003**, *46*, 1980-1988; (c) Watanabe, M.; Kazuta, Y.; Hayashi, H.; Yamada, S.; Matsuda, A.; Shuto, S. Stereochemical diversity-oriented conformational restriction strategy. Development of potent histamine H3 and/or H4 receptor antagonists with an imidazolylcyclopropane structure. *J. Med. Chem.* **2006**, *49*, 5587-5596; (d) Watanabe, M.; Kobayashi, T.; Hirokawa, T.; Yoshida, A.; Ito, Y.; Yamada, S.; Orimoto, N.; Yamasaki, Y.; Arisawa, M.; Shuto, S. Cyclopropane-based stereochemical diversity-oriented conformational restriction strategy: histamine H3 and/or H4 receptor ligands with the 2,3-methanobutane backbone. *Org. Biomol. Chem.* **2012**, *10*, 736-745.

15. Yoshida, K.; Yamaguchi, K.; Sone, T.; Unno, Y.; Asai, A.; Yokosawa, H.; Matsuda, A.; Arisawa, M.; Shuto, S. Synthesis of 2,3- and 3,4-methanoamino acid equivalents with stereochemical diversity and their conversion into the

tripeptide proteasome inhibitor belactosin a and its highly potent cis-cyclopropane stereoisomer. *Org. Lett.* **2008**, *10*, 3571-3574.

16. Adams, J.; Behnke, M.; Chen, S.; Cruickshank, A. A.; Dick, L. R.; Grenier, L.; Klunder, J. M.; Ma, Y. T.; Plamondon, L.; Stein, R. L. Potent and selective inhibitors of the proteasome: dipeptidyl boronic acids. *Bioorg. Med. Chem. Lett.* **1998**, *8*, 333-338.

17. (a) Demo, S. D.; Kirk, C. J.; Aujay, M. A.; Buchholz, T. J.; Dajee, M.; Ho, M. N.; Jiang, J.; Laidig, G. J.; Lewis, E. R.; Parlati, F.; Shenk, K. D.; Smyth, M. S.; Sun, C. M.; Vallone, M. K.; Woo, T. M.; Molineaux, C. J.; Bennett, M. K. Antitumor Activity of PR-171, a Novel Irreversible Inhibitor of the Proteasome. *Cancer Res.* **2007**, *67*, 6383-6391; (b) Kuhn, D. J.; Chen, Q.; Voorhees, P. M.; Strader, J. S.; Shenk, K. D.; Sun, C. M.; Demo, S. D.; Bennett, M. K.; van Leeuwen, F. W.; Chanan-Khan, A. A.; Orlowski, R. Z. Potent activity of carfilzomib, a novel, irreversible inhibitor of the ubiquitin-proteasome pathway, against preclinical models of multiple myeloma. *Blood* **2007**, *110*, 3281-3290.

18. Yoshida, K.; Yamaguchi, K.; Mizuno, A.; Unno, Y.; Asai, A.; Sone, T.; Yokosawa, H.; Matsuda, A.; Arisawa, M.; Shuto, S. Three-dimensional structure-activity relationship study of belactosin A and its stereo- and regioisomers: development of potent proteasome inhibitors by a stereochemical diversity-oriented strategy. *Org. Biomol. Chem.* **2009**, *7*, 1868-1877.

19. (a) Kazuta, Y.; Matsuda, A.; Shuto, S. Development of Versatile cis- and trans-Dicarbon-Substituted Chiral Cyclopropane Units: Synthesis of (1S,2R)- and (1R,2R)-2-Aminomethyl-1-(1H-imidazol-4-yl)cyclopropanes and Their Enantiomers as Conformationally Restricted Analogues of Histamine. *J. Org. Chem.* **2002**, *67*, 1669-1677; (b) Watanabe, M.; Hirokawa, T.; Kobayashi, T.; Yoshida, A.; Ito, Y.; Yamada, S.; Orimoto, N.; Yamasaki, Y.; Arisawa, M.; Shuto, S. Investigation of the bioactive conformation of histamine H3 receptor antagonists by the cyclopropylic strain-based

conformational restriction strategy. *J. Med. Chem.* **2010**, *53*, 3585-3593.

20. Armstrong, A.; Scutt, J. N. Total synthesis of (+)-belactosin A. *Chem. Commun.* **2004**, 510-511.

21. (a) Charette, A. B.; Juteau, H. Design of Amphoteric Bifunctional Ligands - Application to the Enantioselective Simmons-Smith Cyclopropanation of Allylic Alcohols. *J Am Chem Soc* **1994**, *116*, 2651-2652; (b) Charette, A. B.; Juteau, H.; Lebel, H.; Molinaro, C. Enantioselective cyclopropanation of allylic alcohols with dioxaborolane ligands: Scope and synthetic applications. *J Am Chem Soc* **1998**, *120*, 11943-11952.

22. The IC50 values of 3a and belactosin A were relatively higher than those reported previously (ref. 18) because of the different assay procedures.

23. Arastu-Kapur, S.; Anderl, J. L.; Kraus, M.; Parlati, F.; Shenk, K. D.; Lee, S. J.; Muchamuel, T.; Bennett, M. K.; Driessen, C.; Ball, A. J.; Kirk, C. J. Nonproteasomal Targets of the Proteasome Inhibitors Bortezomib and Carfilzomib: a Link to Clinical Adverse Events. *Clin. Cancer Res.* **2011**, *17*, 2734-2743.

24. Muchamuel, T.; Basler, M.; Aujay, M. A.; Suzuki, E.; Kalim, K. W.; Lauer, C.; Sylvain, C.; Ring, E. R.; Shields, J.; Jiang, J.; Shwonek, P.; Parlati, F.; Demo, S. D.; Bennett, M. K.; Kirk, C. J.; Groettrup, M. A selective inhibitor of the immunoproteasome subunit LMP7 blocks cytokine production and attenuates progression of experimental arthritis. *Nat. Med.* **2009**, *15*, 781-787.

25. Honda, R.; Tanaka, H.; Yasuda, H. Oncoprotein MDM2 is a ubiquitin ligase E3 for tumor suppressor p53. *FEBS Lett.* **1997**, *420*, 25-27.

26. (a) Levine, A. J. p53, the Cellular Gatekeeper for Growth and Division. *Cell* **1997**, *88*, 323-331; (b) Vogelstein, B.; Lane, D.; Levine, A. J. Surfing the p53 network. *Nature* **2000**, *408*, 307-310; (c) Vousden, K. H.; Lu, X. Live or let die: the cell's response to p53. *Nat. Rev. Cancer* **2002**, *2*, 594-604; (d) Oren, M. Decision making by p53: life, death and cancer. *Cell*

Death Differ. **2003**, *10*, 431-442.

27. (a) Duriez, P. J.; Shah, G. M. Cleavage of poly(ADP-ribose) polymerase: a sensitive parameter to study cell death. *Biochem. Cell Biol.* **1997**, *75*, 337-349; (b) Kaufmann, S. H.; Desnoyers, S.; Ottaviano, Y.; Davidson, N. E.; Poirier, G. G. Specific Proteolytic Cleavage of Poly(ADP-ribose) Polymerase: An Early Marker of Chemotherapy-induced Apoptosis. *Cancer Res.* **1993**, *53*, 3976-3985.

28. Williamson, M. J.; Blank, J. L.; Bruzzese, F. J.; Cao, Y.; Daniels, J. S.; Dick, L. R.; Labutti, J.; Mazzola, A. M.; Patil, A. D.; Reimer, C. L.; Solomon, M. S.; Stirling, M.; Tian, Y.; Tsu, C. A.; Weatherhead, G. S.; Zhang, J. X.; Rolfe, M. Comparison of biochemical and biological effects of ML858 (salinosporamide A) and bortezomib. *Mol. Cancer Ther.* **2006**, *5*, 3052-3061.

29. Groll, M.; Huber, R.; Potts, B. C. M. Crystal Structures of Salinosporamide A (NPI-0052) and B (NPI-0047) in Complex with the 20S Proteasome Reveal Important Consequences of β-Lactone Ring Opening and a Mechanism for Irreversible Binding. *J. Am. Chem. Soc.* **2006**, *128*, 5136-5141.

30. Kupperman, E.; Lee, E. C.; Cao, Y.; Bannerman, B.; Fitzgerald, M.; Berger, A.; Yu, J.; Yang, Y.; Hales, P.; Bruzzese, F.; Liu, J.; Blank, J.; Garcia, K.; Tsu, C.; Dick, L.; Fleming, P.; Yu, L.; Manfredi, M.; Rolfe, M.; Bolen, J. Evaluation of the Proteasome Inhibitor MLN9708 in Preclinical Models of Human Cancer. *Cancer Res.* **2010**, *70*, 1970-1980.

Table of Contents graphic.

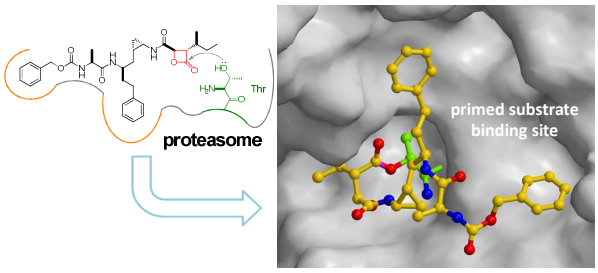

IC_{50} = 5.7 nM